International Journal of Thermal Sciences 48 (2009) 1319–1326

Contents lists available at ScienceDirect

International Journal of Thermal Sciences

www.elsevier.com/locate/ijts

Turbulent forced convection flow adjacent to inclined forward step in a duct

S.A. Gandjalikhan Nassab [a,*], R. Moosavi [b], S.M. Hosseini Sarvari [c]

[a] *Mechanical Engineering Department, Shahid Bahonar University, Kerman, Iran*
[b] *Mechanical Engineering Department, Yasouj University, Yasouj, Iran*
[c] *Mechanical Engineering Department, Sistan and Baluchestan University, Zahedan, Iran*

ARTICLE INFO

Article history:
Received 5 January 2008
Received in revised form 11 October 2008
Accepted 14 October 2008
Available online 31 October 2008

Keywords:
Turbulent forced convection
Forward facing step
Schwarz–Christoffel transformation

ABSTRACT

To calculate complex turbulent flows with heat transfer, we have developed a numerical procedure to solve the governing equations based on the orthogonal grids generation by the Schwarz–Christoffel transformation. In the present work, the turbulent fluid flow over a single forward facing step is studied to examine the effects of step length and its inclination angle on flow and heat transfer distributions. The continuity, Navier–Stokes and energy equations are solved numerically and the k–ε model is employed for computation of turbulence fluctuations. Because of the complex flow geometry, the governing equations are transformed in the computational domain and the discretized forms of these equations are obtained with finite volume method and solved by the SIMPLE Algorithm. The present results reveal that the coefficient of heat transfer and also the hydrodynamic behavior of the flow are strongly dependent to step length and inclination angle.

1. Introduction

In a variety of practical engineering such as power generating equipments and in cooling of electronic devices, separating and reattaching flows occur because of sudden changes in flow geometry. The fluid flows over forward and backward steps which can be found in many engineering systems are good examples. A great deal of mixing of high and low fluid energy occurs in the recirculation region has a considerable effect on the flow and heat transfer performance of these devices. For example, the maximum convective heat transfer coefficient and minimum wall shear stress take place in the neighborhood of reattaching flow region, while the minimum heat transfer occurs at the corner. Therefore, the studies on separated flows both theoretically and experimentally have been conducted extensively during the past decade, and the fluid flow over backward step received most of the attention. Although this geometry is very simple, but the heat transfer and fluid flow over this type of step contain most of complexities. Consequently, it has been used in the benchmark investigations. In the benchmark problem, a steady-state two-dimensional mixed convection laminar flow in a vertical channel with a backward-facing step was solved. By now, more than ten papers were contributed in which the benchmark problem was solved numerically by different methods [1].

A review of research on laminar mixed convection flow over forward- and backward-facing steps was done buy Mulaweh [2]. In that work, a comprehensive review of such flows those have been reported in several studies in the open literature was presented. The purpose was to give a detailed summary of the effect of several parameters such as step height, Reynolds number, Prandtl number and the buoyancy force on the flow and thermal fields downstream of the step. Several correlation equations were also summarized in that review.

There are several works in which the turbulent flows with heat transfer over forward- and backward-facing steps were studied theoretically. The governing equations for the thermodynamically consistent rate-dependent turbulent model were briefly reviewed by Chowdhury and Ahmadi [3]. The requirements of the model were incorporated in a computer code (STARPIC-RATE) which is the advanced version of TEACH code. The model leaded to an anisotropic effective viscosity and was capable of predicting the expected turbulent stresses. The computational model was used to simulate the mean turbulent flow fields behind a plane backward-facing step in a channel, and good results were obtained.

A new turbulent model for predicting flow and heat transfer in separating and reattaching flows was introduced by Abe et al. [4,5]. The model was modified from the latest low-Reynolds number k–ε model, such that the main improvement was achieved by introduction of the Kolmogorov velocity scale, $u_c = (\nu\varepsilon)^{1/4}$ instead of the friction velocity, to account for the near-wall and low-Reynolds number effects in both attached and detached flows. After investigating the characteristics of various time scales for the heat transfer model, they adopted a composite time scale which gives weight to a shorter scale among the velocity- and temperature-field time scales. The model predicted quite successfully the separating and

* Corresponding author.
E-mail address: ganjali2000@yahoo.com (S.A. Gandjalikhan Nassab).

1290-0729/$ – see front matter
doi:10.1016/j.ijthermalsci.2008.10.003

Nomenclature

A, B	constant parameters
a	length of bottom wall before the step
b	length of bottom wall after the step
c_μ, $c_{\varepsilon 1}$, $c_{\varepsilon 2}$	model constant = 0.09, 1.44 and 1.92, respectively
D_h	hydraulic diameter
h	convection coefficient
H	duct's height
J	Jacobian of transformation
k	turbulent kinetic energy
K	thermal conductivity
L	duct's length
n	normal direction to solid surface
N	number of polygon apices
Nu	Nusselt number $= hH/K$
p	pressure
P_k	turbulent generation rate
Pr	Prandtl number
Re	Reynolds number $= \rho U H/\mu$
S	step's length
S_φ	source term
T_c	fluid temperature at duct's inlet
t	temperature fluctuation
T	fluid temperature
T_h	temperature of heated walls region
U	fluid inlet velocity
U_i, u_i	mean velocity and turbulent fluctuation in i-direction
$\overline{u_i u_j}$	Reynolds stress tensor
$\overline{u_i t}$	turbulent heat flux tensor
(x, y)	coordinates in physical plane
Z	physical plane
ν	kinematic viscosity
ν_t	turbulent kinematic viscosity
γ	computational domain
α	angle of rotation
(ξ, η)	coordinates in computational plane
φ	dependent variables
Γ_φ	coefficient of diffusive terms in Eq. (12)
θ	step inclined angle
ε	dissipation rat
δ_{ij}	Kronecker delta
σ_k, σ_ε, σ_θ	model constants = 1, 1.3 and 0.9, respectively

Subscripts

i, j	1 and 2 denote x- and y-directions, respectively
fd	fully developed
in	inlet

reattaching turbulent flows with heat transfer downstream of a backward-facing step.

In a recent study, Yilmaz and Oztop [6] examined the turbulence forced convection heat transfer over double forward facing step in 2006. The Navier–Stokes and energy equations were solved numerically by CFD techniques. The solutions were obtained using the commercial FLUENT code which uses the finite volume method. Effects of step heights, step lengths and the Reynolds number on heat transfer and fluid flow were investigated. Results showed that the second step can be use as a control device for both heat transfer and fluid flow.

There are many publications in literature that experimentally studied the effects of sudden contraction and expansion on characteristics of flow and heat transfer in turbulent condition. Han and Park [7] studied developing turbulent heat transfer in a rectangular channel with a sudden contraction at inlet and ribs along two opposite walls. All geometrical dimensions were consistent with those found in the cooling passages of gas turbine blades. They showed that flow separation and reattachment at, and downstream of, the channel contraction resulted in high heat transfer levels. Liou and Hwang [8] investigated local heat transfer characteristics of developing turbulent flow in a rectangular duct with an abrupt contraction entrance. They showed that separation at the duct inlet plays an important role in the axial distribution of the heat transfer coefficient in the thermal entrance region. The effects of backward- and forward-facing steps on turbulent natural convection along a vertical flat plate were examined experimentally by Mulaweh [9]. Laser-Doppler velocimeter and cold wire anemometer were used to measure simultaneously the time-mean turbulent velocity and temperature distributions and their turbulent fluctuation intensities. Results revealed that the maximum local Nusselt number occurs in the vicinity of the reattachment region and it is approximately twice for the case of backward-facing step and two and half times for the case of forward-facing step, than that of the flat plate value at similar flow and thermal conditions.

In all of the above references, the step in both forward and backward cases was vertical to the stepped wall. In these geometries, there is a sudden expansion or contraction in the flowing flow. But, there are several applications in which the flow geometry expands or contracts gradually, such as turbine blade cooling, combustion chambers, transition duct connection and atmospheric flows over fences and hills. There are few works in analyzing fluid flow with heat transfer over inclined surfaces. Besides, in those works, the fluid flow was assumed to be laminar. For example, the three-dimensional convection flow over an inclined backward-facing step in a rectangular duct was studied by Chen et al. [10]. The bottom wall was heated with constant heat flux, while other walls were maintained as being thermally adiabatic. Numerical solution of the governing equations for laminar flow was performed by utilizing SIMPLE Algorithm for the pressure calculations. In the computations, the step length was maintained as constant while its inclination angle was changed from 15° to 90°. As a main result, it was found that the location of maximum Nusselt number is closely associated with the location where the negative transverse velocity component is maximum.

To the best of authors' knowledge, the turbulent forced convective heat transfer over inclined forward- and backward-facing steps has not been investigated numerically and the present contribution is the first such study. The objective of the present paper is twofold. First, is to present a CFD technique based on the grid generation by the Schwarz–Christoffel transformation in simulating two-dimensional turbulent flows. Second, is to analyze the turbulent flow over inclined step in a duct with heat transfer in order to determine the hydrodynamic and thermal behavior of this type of convective flow. Thereby, the present work deals with the numerical solution of the governing equations to determine the fluid flow and temperature distributions of a forced convection turbulent flow over a forward inclined step, and the effects of inclined angle and the step length on the fluid flow and heat transfer are thoroughly explored. Because of the complex flow geometry, the governing equations are transformed into the computational domain and the Schwarz–Christoffel transformation is used to generate orthogonal grids. The finite difference forms of the transformed equations are obtained with finite volume method and solved by the SIMPLE Algorithm.

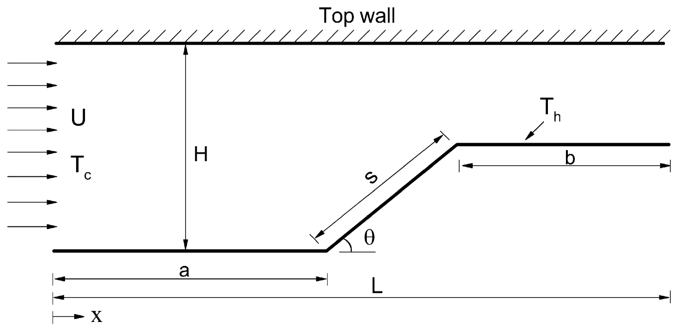

Fig. 1. Physical model.

2. Model description

Two-dimensional turbulent forced convection flow in a heated rectangular duct with an inclined forward-facing step is numerically simulated. A schematic of the physical domain is shown in Fig. 1. The channel consists of top and bottom walls with an inclined step with length S and inclination angle θ. Top wall is adiabatic and bottom walls and step are heated with uniform temperature. Lengths of bottom walls are depicted by a and b and the duct's height and length are H and L, respectively. The duct's height (H) is considered as the characteristic length in the computation. Fluid enters into the duct with uniform temperature of T_c and the heated surfaces are maintained at a uniform temperature T_h.

3. Flow equations

3.1. Mean flow equations

For a steady incompressible two-dimensional turbulent flow, the conservations of mass, momentum and energy may be written as:

Continuity

$$\frac{\partial U_j}{\partial x_j} = 0 \tag{1}$$

Momentum

$$\frac{\partial (U_j U_i)}{\partial x_j} = -\frac{1}{\rho}\frac{\partial P}{\partial x_i} + \frac{\partial}{\partial x_j}\left(\nu \frac{\partial U_i}{\partial x_j} - \overline{u_i u_j}\right) \tag{2}$$

Energy

$$\frac{\partial (U_j T)}{\partial x_j} = \frac{\partial}{\partial x_j}\left(\frac{\nu}{Pr}\frac{\partial T}{\partial x_j} - \overline{u_j t}\right) \tag{3}$$

3.2. Turbulence model equations

The turbulence model employed for flow simulation is the standard zonal k–ε model (Bo et al. [11]). In this turbulence model, the Reynolds stresses and heat fluxes are obtained via the eddy-viscosity and eddy-diffusivity approximations, respectively:

$$\overline{u_i u_j} = -\nu_t\left(\frac{\partial U_i}{\partial x_j} + \frac{\partial U_j}{\partial x_i}\right) + \frac{2}{3}\delta_{ij}k \tag{4}$$

$$\overline{u_i t} = -\frac{\nu_t}{\sigma_\theta}\frac{\partial T}{\partial x_i} \tag{5}$$

and the turbulent viscosity, ν_t, is given by

$$\nu_t = c_\mu \frac{k^2}{\varepsilon} \tag{6}$$

In which the turbulent kinetic energy k, and turbulent dissipation rate ε are obtained based on the standard k–ε model from the following transport equations:

$$\frac{\partial}{\partial x_j}(U_j k) = \frac{\partial}{\partial x_j}\left[\left(\frac{\nu_t}{\sigma_k}\right)\frac{\partial k}{\partial x_j}\right] + P_k - \varepsilon \tag{7}$$

$$\frac{\partial}{\partial x_j}(U_j \varepsilon) = \frac{\partial}{\partial x_j}\left[\left(\frac{\nu_t}{\sigma_\varepsilon}\right)\frac{\partial \varepsilon}{\partial x_j}\right] + c_{\varepsilon 1}\frac{\varepsilon}{k}P_k - c_{\varepsilon 2}\frac{\varepsilon^2}{k} \tag{8}$$

Where P_k which is the generation rate of turbulent kinetic energy can be computed from Eq. (9)

$$P_k = -\overline{u_i u_j}\frac{\partial U_i}{\partial x_j} \tag{9}$$

3.3. Boundary conditions

In the numerical solution of governing equations, the following boundary conditions in the physical plane are considered:

1. At the duct's inlet section, it is assumed that the fluid flow has a uniform velocity distribution equal to U. It is clear that at inlet section, the turbulent kinetic energy and dissipation rate are specified from the experimental condition. In the present computations, the values of k and ε are assumed to be as follows:

   $k = 0.001U^2, \quad \varepsilon = C_\mu k^2/\nu_t, \quad \text{where } \nu_t/\nu = 10$
2. At the duct's outlet section, a zero gradient in stream-wise direction is considered for all dependent variables.
3. On the solid walls, no slip condition is employed, the turbulent kinetic energy is equated to zero and dissipation rate is computed by [4]:

   $$\varepsilon = 2\nu(\partial\sqrt{k}/\partial n)^2 \tag{10}$$

   in which n stands for normal direction to the solid surface.

4. Grid generation

The numerical solution of many problems consists in discretizing the region upon which the governing equations are solved by numerical techniques such that the approximate forms of the conservation equations can give an estimate for the field variables. If the method used to obtain the solution is the finite volume method, it is common and better to use orthogonal grids. The grid generation in the present work is based on the numerical integration of the Schwarz–Christoffel transformation. By this transformation, a polygon in the $z(x, y)$-plane, is mapped onto the upper half of $\gamma(\xi, \eta)$-plane as shown in Fig. 2.

The relation between the z-plane as physical domain to the γ-plane as computational domain is as follows:

$$\frac{dz}{d\gamma} = A\prod_{n=1}^{N}(\gamma - \xi_n)^{-\alpha_n/\pi} \tag{11}$$

In the above equation, α_n is the angle of counterclockwise rotation at each apex and N is the number of polygon apices. The points ξ_n are positions on the real axis in γ-plane, where each of them corresponds to an apex of the polygon in z-plane. The values of parameters ξ_n are unknown which may be determined iteratively during the numerical calculations. A is a complex constant that depends on the geometry of physical domain. According to Riemann theorem [12], the positions of three points of ξ_n are arbitrary. The mapping functions of $z(\gamma)$ may be obtained by integration of Eq. (11) as follows:

$$z(\gamma) = A\int_{\gamma_0}^{\gamma}\prod_{n=1}^{N}(\gamma - \xi_n)^{-\alpha_n/\pi}\,d\gamma + B \tag{12}$$

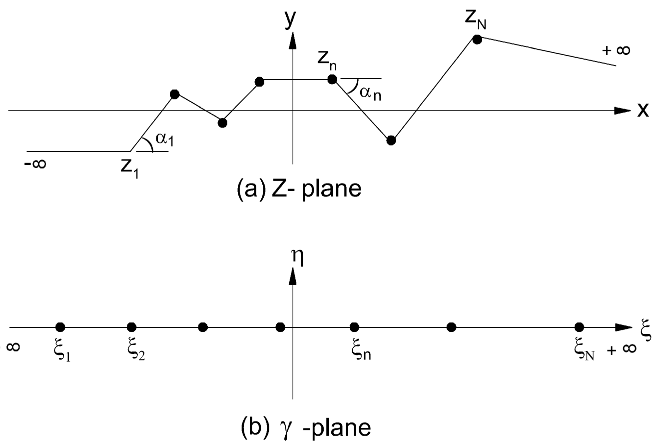

Fig. 2. Mapping of a polygon in $z(x, y)$-plane onto the upper half of $\gamma(\xi, \eta)$-plane.

where γ_0 is a point on the upper half of γ-plane, and B is a complex constant. The correct selection of points ξ_n involves an iterative procedure. The details of this transformation and the related numerical procedure are given in Refs. [13] and [14]. By this technique, the relation between physical and computational planes is determined from which the values of metric coefficients which are needed to transform the governing equations into computational domain can be obtained. The transformed form of the governing equations in the computational plane for any dependent variable Ψ, can be written in the following common form:

$$\frac{\partial}{\partial \xi}\left[JA'\Psi - \Gamma_\Psi \frac{\partial \Psi}{\partial \xi}\right] + \frac{\partial}{\partial \eta}\left[JB'\Psi - \Gamma_\Psi \frac{\partial \Psi}{\partial \eta}\right] = S_\Psi \tag{13}$$

in which the values of A', B', Ψ, Γ_Ψ and S_Ψ are different at each governing equation.

5. Solution procedure

Because of the complex geometry in the physical domain, the governing equations were transformed into a simple rectangular computational plane. The transformed forms of these equations have a common form as was presented in Eq. (13). These partial differential equations were made discrete by integrating over an elemental cell volume. The staggered type of control volumes were used for the ξ- and η-velocity components and other variables of interest were computed at the grid nodes. The discretized forms of the governing equations were solved by the SIMPLE Algorithm of Patankar and Spalding [15]. Numerical solutions were obtained iteratively by the line-by-line method until the converged solution was obtained. The convergence was assumed to have been achieved when sum of the absolute residuals did not exceed 10^{-4} for each equation. To reach this goal, 3000 to 3500 iterations were required depending to the flow and geometrical conditions.

Numerical calculations were coded into a computer program in FORTRAN. For each test case, the influence of grid refinement on flow and heat transfer predictions is determined. Based on the grid-independent study, the optimum grids with 300 to 500 intervals in the ξ-direction and 100 to 150 intervals in the η-direction dependent to the flow condition and geometry were employed for the numerical analysis along with clustering near to the solid boundaries and closed to the domains with sharp gradients in dependent variables.

6. Results and discussion

First, in order to validate the applied method, several test cases of turbulent flows are analyzed and the results are compared with experimental and theoretical results of others. In the first test case, the turbulent flow over a backward-facing step in a duct is simulated and the distribution of x-component of fluid mean velocity downstream the step at $x = 10.1$ cm is shown in Fig. 3. Also, a comparison is made with experiment. In the experimental study by Kim et al. [16], air flow entered to the duct with uniform velocity of $U_{in} = 18.2$ m/s and the duct heights were equal to 7.62 and 11.43 cm before and after the step, respectively. It should be noted that because the step is vertical to the stepped wall in this test case, the governing equations were solved directly in the physical (x, y)-plane.

Fig. 3 indicates that the axial section $x = 10.1$ cm is located in the recirculation zone such that the fluid velocity is negative in the region near the wall. However, the model predictions for the mean velocity appear to be in good agreement with experiment.

In the second test case, turbulent flow in a channel with sudden contraction is examined and the computed local Nusselt number is shown in Fig. 4 and a comparison is made with experimental

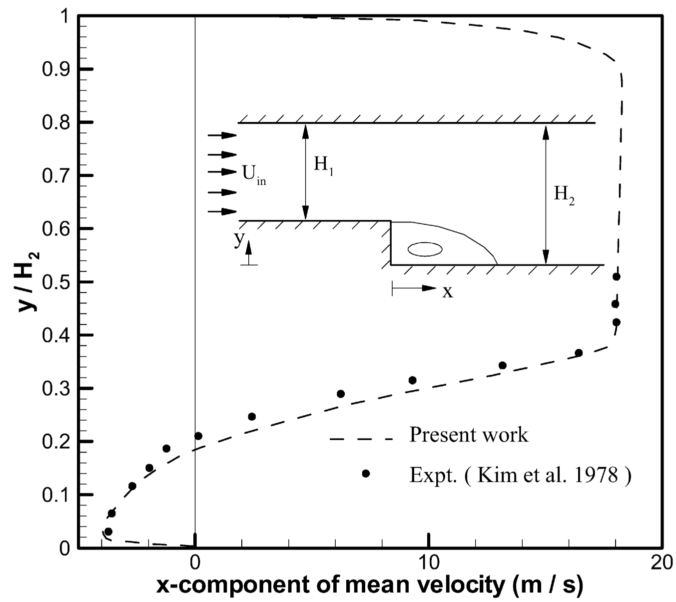

Fig. 3. Distribution of mean velocity across the duct.

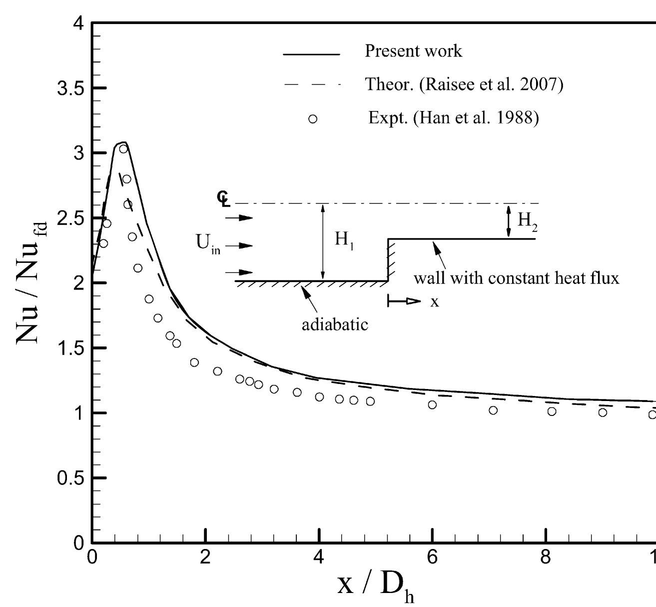

Fig. 4. Predicted local Nusselt number.

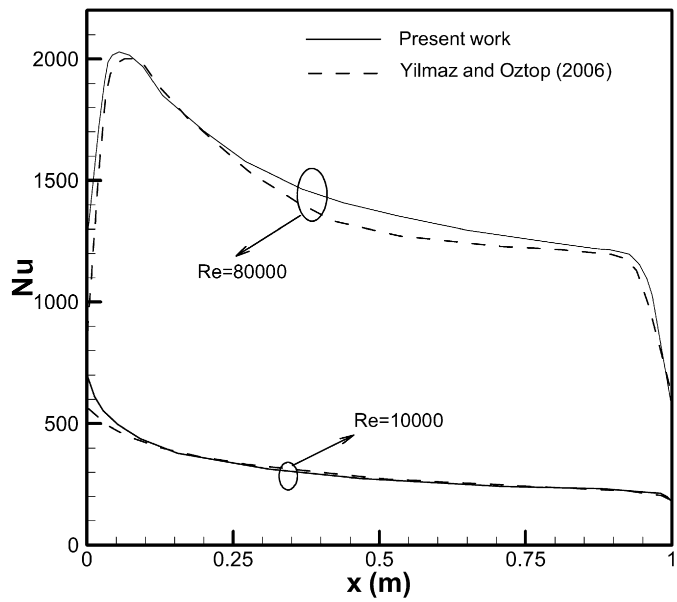

Fig. 5. Local Nusselt number along the heated wall at two different *Re* (case 8 of Ref. [6]).

data by Han et al. [7]. The contraction ratio is 3.75, the value of Reynolds number based on the hydraulic diameter is 30 000 and the walls after the step are heated at constant heat flux, while other surfaces are adiabatic. It is seen in Fig. 4 that as a result of flow separation immediately at the channel contraction, the value of heat transfer coefficient increases because of the recirculation zone up to the reattached point. This point is positioned on the wall about half one hydraulic diameter downstream of the channel contraction. After the reattachment point, the flow builds up a new boundary layer as it develops along the channel with decrease in the value of Nusselt number. Agreements between the present result with experiment and also with theoretical results by Raisee et al. [17] are satisfactory. It should be noted that in Ref. [17], a linear low *Re* k–ε model was employed for calculating the Reynolds stresses and turbulent heat flux.

In the third test case, turbulent flow with heat transfer over two forward right angle steps in a duct is simulated and the numerical results are compared with those obtained numerically from FLUENT code by Yilmaz and Oztop [6]. In Fig. 5, the computed local Nusselt numbers on the bottom wall upstream the step at two different Reynolds number are compared with the reported results in Ref. [6]. In this case study, the values of geometrical parameters are the same as used in case 8 of Ref. [6] for comparison. The fluid enters into the duct with uniform temperature of 293 K, the bottom wall is heated and has a constant temperature of 313 K, while the top wall and steps are adiabatic. As expected, heat transfer is enhanced with the increasing of *Re*, such that *Nu* decreases along the heated wall. However, a good consistency is seen between the present results and those obtained in Ref. [6].

Henceforth, considering the results of these three test cases, it can be concluded that the applied CFD techniques with the present grid generation method based on the Schwarz–Christoffel transformation are valid in simulation of turbulent flows.

As it was mentioned before, the numerical technique described in the present work was used to simulate the fluid flow over an inclined step in a duct with heat transfer. Numerical simulations have been performed for air flow and the values of parameters in the related test cases are given in Table 1.

The fluid flow with heat transfer over an inclined forward step in a duct with $\theta = 80°$ is simulated as another case study in the present work. The streamlines with the values of stream function,

Table 1
Values of parameters in flow over inclined step.

Parameters	Units	Values
a	m	1
H	m	0.15
L	m	1.6
S	m	0.0225, 0.0525, 0.105
θ	–	20°, 50°, 70°, 80°
T_c	K	298
T_h	K	320
Pr	–	0.71
Re	–	3×10^4, 5×10^4, 8×10^4

the contours of pressure coefficient, isotherms and the distributions of turbulent kinetic energy and dissipation rate in the region $0.6\ \text{m} \leqslant x \leqslant 1.4\ \text{m}$ are shown in Fig. 6. The effect of inclined step on the flow is clearly seen from the curvature of streamlines. Two small recirculation zones near to the step corners are seen in this figure. About the contours of pressure which are plotted in Fig. 6b, it is seen that in the vicinity of the duct's inlet section, the pressure contours are almost vertical to the bottom and top walls up to the step, which indicates that the fluid flow becomes hydrodynamically developed at that region. The same behavior is seen near to the outlet section of the channel. It is seen that as the fluid moves toward the step surface which behaves as an obstacle, pressure increases and on the bottom wall after the step, there is a sharp decrease in fluid pressure because the existence of recirculation zone. Finally, downstream of the step, the fluid pressure decreases in the flow direction because of the friction. Isotherms are plotted in Fig. 6c. Since, the bottom wall and step are heated with uniform temperature of $T_h = 320$ K, isotherms are almost parallel to these surfaces such that the value of fluid temperature decreases normal to the heated surfaces. Contours of turbulent kinetic energy (TKE) and dissipation rate are plotted in Figs. 6d and 6e. As these figures show, TKE has small values near to the solid boundaries and in the region far from the step. The maximum value of this parameter occurs at the vicinity of the step surface where TKE has a complex variation. Also, it is seen that near to the step, there is a region with large dissipation rate.

The variation of convection coefficient on the bottom wall including the step surface is shown in Fig. 7. The convection coefficient is expressed along the no-dimensional group of Nusselt number which is defined as $Nu = hH/K$. Fig. 7 indicates the same behavior for the variation of *Nu* before the step as predicted in Ref. [6] which was shown in Fig. 5. Such that, after a small increase in Nusselt number in the vicinity of duct's inlet section, the convection coefficient decreases along the flow direction. On the step surface, the impact of the relatively cooler fluid on the step heated surface increases the value of local *Nu*, sharply. This increasing is continued and the maximum value of heat transfer coefficient occurs in the vicinity of reattachment zone where the velocity and temperature fluctuations have maximum values. Then, the local Nusselt number decreases as the distance continues to increase in the streamwise direction.

In order to study the effect of step inclined angle on the heat transfer distribution, the numerical solutions of the governing equations were obtained for different values of θ. The effects of inclination angle on the variations of Nusselt number on both bottom walls before and after the step are presented separately in Figs. 8 and 9. Such that in Fig. 8, the variation of *Nu* on the bottom wall before the step which is located in the region $0 \leqslant x \leqslant 1$ m is shown. From this figure, it is seen that the step inclined angle θ does not have a considerable effect on the convection heat transfer upstream the step. It is due to this fact that for high convective flow, significant influences travel only from upstream to downstream, thus makes the space coordinate nearly one-way.

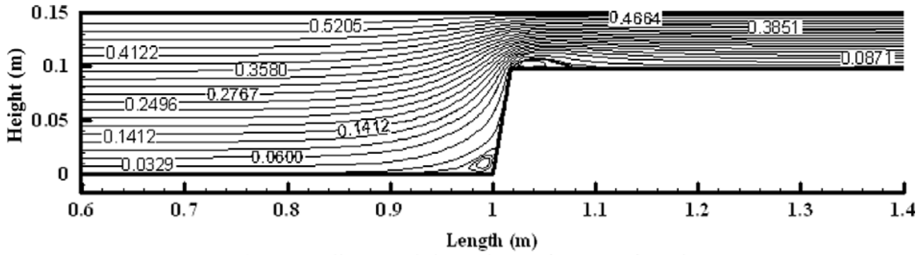

(a) Streamlines and the values of stream function

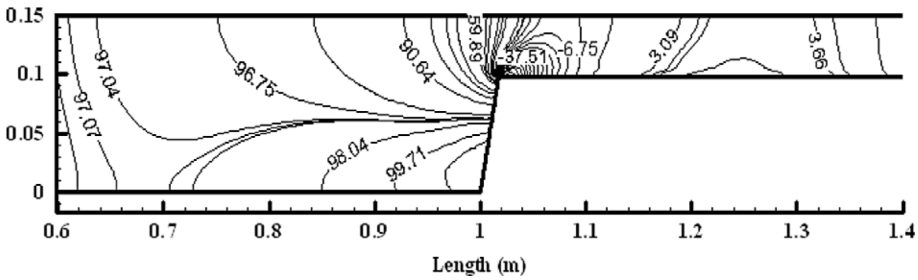

(b) Pressure coefficient

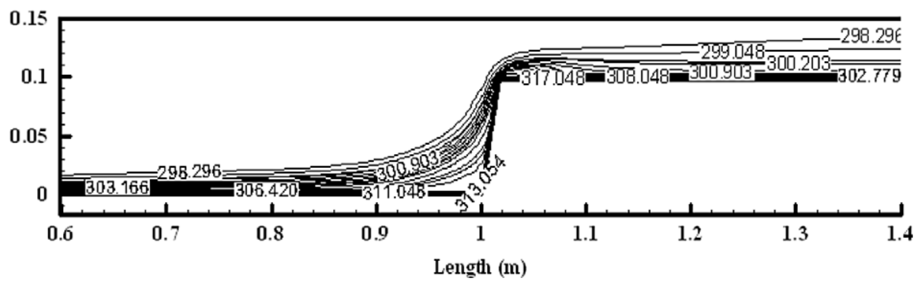

(c) Isotherms

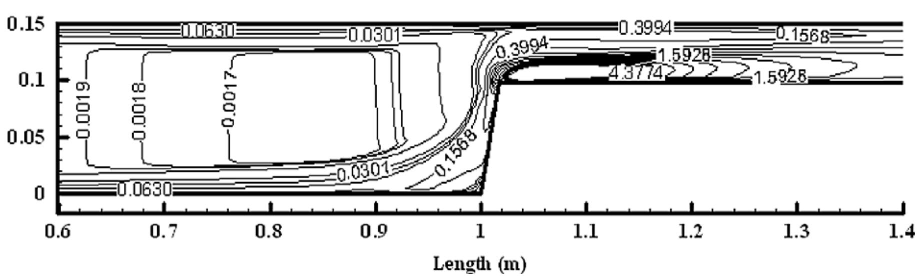

(d) Turbulent kinetic energy

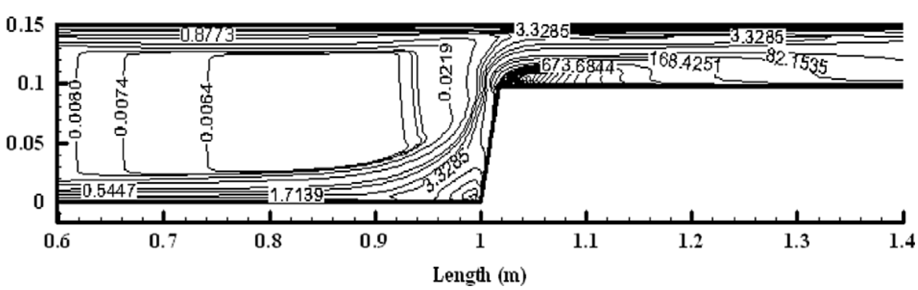

(e) Dissipation Rate

Fig. 6. Streamlines, contours of pressure coefficient, isotherms, turbulent kinetic energy and dissipation rate. $\theta = 80^\circ$, $S/H = 0.7$, $Re = 30\,000$.

The distributions of Nusselt number on the bottom wall downstream of the step at three different values of θ and two different values of *Re* are shown in Fig. 9. Because of the constant step length, the starting points of the curves in this figure move toward the upstream direction for higher values of the inclined angle. Different trends for the variation of *Nu* are seen at different values of θ. In the cases with $\theta = 80^\circ$ those have large vortices and high turbulence fluctuations after the flow separation in the recirculation zone, the impact of the relatively cooler fluid from the shear layer on the heated wall and the deflection of cooler fluid into the recirculating flow region cause a rapid increase in the Nusselt number. The maximum values of *Nu* occur in the vicinity of reattachment point where the velocity and temperature fluctuations have great values. Then, the local Nusselt number decreases as the distance continues to increase in downstream direction. But for $\theta = 50^\circ$, which has the vortices with low intensities in the recirculation zone in comparison to the case of $\theta = 80^\circ$, the local Nusselt number first decreases to a minimum value in a short dis-

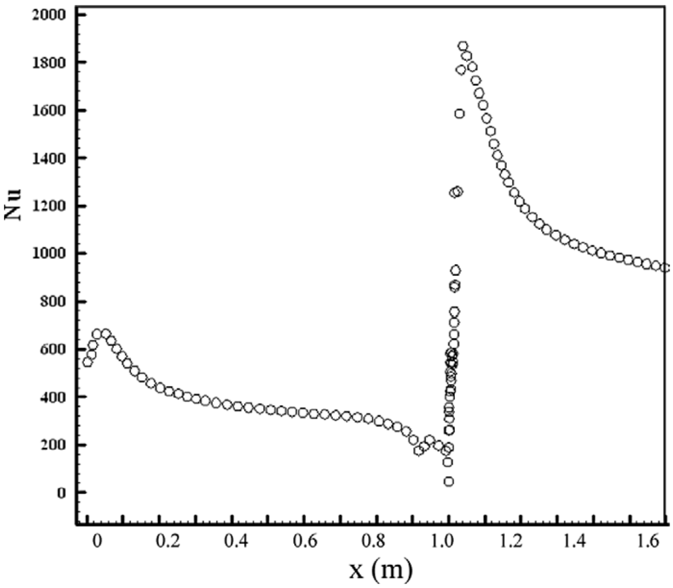

Fig. 7. Distribution of local Nusselt number along the duct. $\theta = 80°$, $S/H = 0.7$, $Re = 30\,000$.

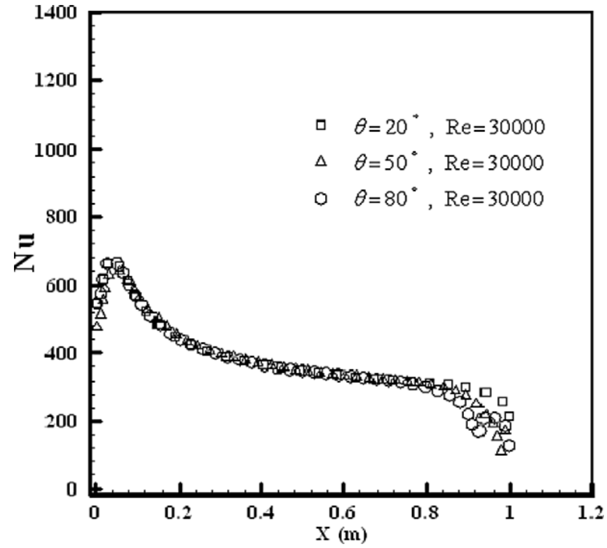

Fig. 8. Distribution of Nusselt number along the heated wall before the step. $S/H = 0.7$, $Re = 30\,000$.

tance after the flow separation. It is due to the low rate of mixing of high and low fluid energies just after the separation. Then, the local Nusselt number increases up to a maximum value at the reattached point after which, the Nusselt number decreases along the flow direction. Finally, for the case of $\theta = 20°$ in which there is not any separated flow, the local Nusselt number decreases in all parts of the bottom wall. Similar trends for the variation of *Nu* were also reported experimentally by Mulaweh [18] in the flow over right angle forward steps with different heights and theoretically by Marty et al. [19] for the fluid flow over blunt flat plate at different thicknesses. However, Fig. 9 shows that the inclined angle θ has a considerable effect on the wall convection coefficient downstream the step.

The effect of *Re* on convection coefficient is also presented in Fig. 9. Similar trends are seen for the variation of *Nu* at different values of *Re*, such that the value of *Nu* increases with increasing Reynolds number for all values of the inclined angle.

The effect of step length on the local Nusselt number downstream of the step is illustrated in Fig. 10. The variation of *Nu* for each of step length is similar to those shown with $\theta = 50°$ and $20°$ in Fig. 9. Such that, the local Nusselt number first decreases sharply along a very short distance after the step surface, then it increases to a maximum value in the reattached point and finally it decreases along the flow direction up to the outlet section. It is seen that the value of *Nu* increases with increasing step length in all parts of the bottom wall.

7. Conclusion

In this paper, based on the Schwarz–Christoffel transformation in generating orthogonal grids, the turbulent fluid flow with heat

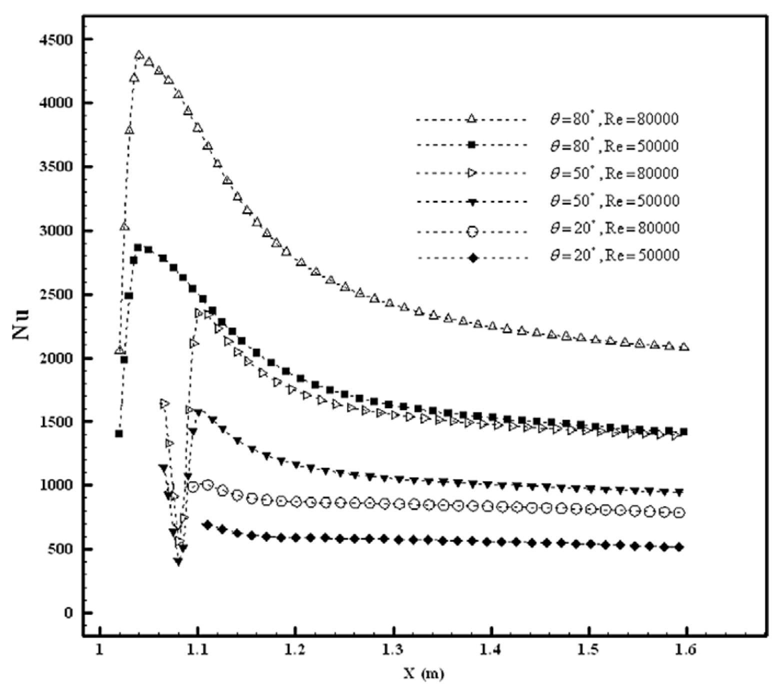

Fig. 9. Distribution of Nusselt number along the heated wall after the step. $S/H = 0.7$.

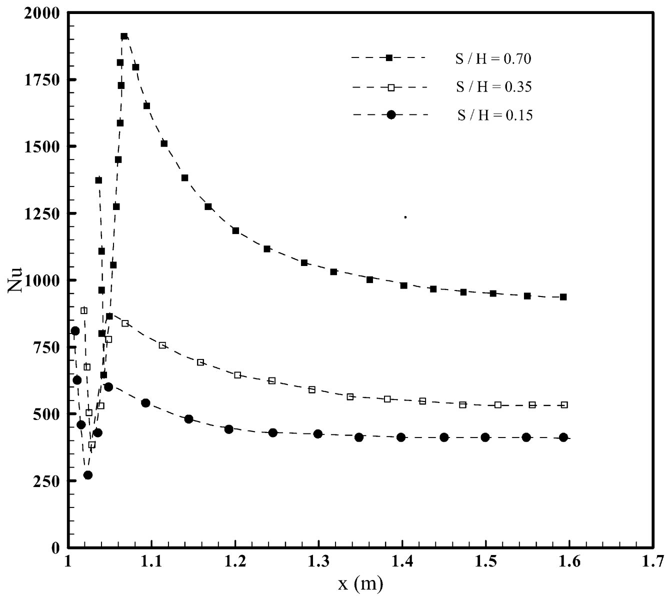

Fig. 10. Effect of step length on convection coefficient. $Re = 30\,000$, $\theta = 70°$.

transfer over an inclined forward-facing step in a duct was investigated. Transformed forms of the governing equations in the computational domain were discretized with finite volume method and solved by the SIMPLE Algorithm. Results including the velocity, pressure, temperature, turbulent kinetic energy, dissipation rate and convection coefficient were presented in this paper. Results show that the step length and inclined angle have great effects on both fluid flow and heat transfer distributions.

References

[1] B.F. Blackwell, B.F. Armaly, Computational aspect of heat transfer benchmark problems, in: ASME Winter Annual Meeting, HTD 258 (1993) 1–20.

[2] H.I.A. Mulaweh, A review of research on laminar mixed convection flow over backward- and forward-facing steps, Int. J. Thermal Sci. 42 (2003) 897–909.

[3] S.J. Chowdhury, G. Ahmadi, A Thermodynamically consistent rate-dependent model for turbulence. Part II. Computational results, Int. J. Non-linear Mechanics 27 (1992) 705–718.

[4] K. Abe, T. Kondoh, Y. Nagano, A new turbulence model for predicting fluid flow and heat transfer in separating and reattaching flows. I. Flow field calculations, Int. J. Heat Mass Transfer 37 (1994) 139–151.

[5] K. Abe, T. Kondoh, Y. Nagano, A new turbulence model for predicting fluid flow and heat transfer in separating and reattaching flows. II. Thermal field calculations, Int. J. Heat Mass Transfer 38 (1994) 1467–1481.

[6] I. Yilmaz, H.F. Oztop, Turbulence forced convection heat transfer over double forward facing step flow, Int. Comm. Heat Mass Transfer 33 (2006) 508–517.

[7] J.C. Han, J.S. Park, Developing heat transfer in rectangular channels with rib turbulators, Int. J. Heat Mass Transfer 31 (1988) 183–195.

[8] T. Liou, J. Hwang, Developing heat transfer and friction in a ribbed rectangular duct with flow separation at inlet, ASME J. Heat Transfer 114 (1992) 565–573.

[9] H.I.A. Mulaweh, Effects of backward- and forward-facing steps on turbulent natural convection flow along a vertical flat plate, Int. J. Thermal Sci. 41 (2002) 376–385.

[10] Y.T. Chen, J.H. Nie, H.T. Hsieh, L.J. Sun, Three-dimensional convection flow adjacent to inclined backward-facing step, Int. J. Heat Mass Transfer 49 (2006) 4795–4803.

[11] T. Bo, H. Lacovides, B.E. Launder, The prediction of convective heat transfer in rotating square ducts, in: 8th Symp. on Turbulent Shear Flows, Munich, Germany, 1991, pp. 24.4.1–24.4.6.

[12] L.M. Milne-Thomson, Theoretical Hydrodynamics, 4th ed., Macmillan, New York, 1960.

[13] S.H. Mansouri, M.A. Mehrabian, S.M. Hosseini Sarvari, Simulation of ideal external and internal flows with arbitrary boundaries using Schwarz–Christoffel transformation, Int. J. Eng., Trans. A 17 (4) (2004) 405–414.

[14] K.P. Sridhar, R.T. Davis, A Schwarz–Christoffel method for generating two-dimensional flow grids, Journal of Fluid Engineering 107 (1985) 330–337.

[15] S.V. Patankar, B.D. Spalding, A calculation procedure for heat, mass and momentum transfer in three-dimensional parabolic flows, Int. J. Heat Mass Transfer 15 (1972) 1787–1806.

[16] J. Kim, S.J. Kline, J.P. Johnston, Investigation of separation and reattachment of a turbulent shear layer: Flow over a backward facing step. Report MD-37, Thermo-Science devision, Dept. of Mech. Engng., Stanford University, 1978.

[17] M. Raisee, S.H. Hejazi, Application of linear and non-linear low-*Re* k–ε models in two-dimensional predictions of convective heat transfer in passages with sudden contractions, Int. J. Heat and Fluid Flow 28 (2007) 429–440.

[18] H.I.A. Mulaweh, Turbulent mixed convection flow over a forward-facing step-the effect of step heights, Int. J. Thermal Sci. 44 (2005) 155–162.

[19] P. Marty, F. Michel, P. Tochon, Experimental and numerical study on the heat transfer along a blunt flat plate, Int. J. Heat Mass Transfer 51 (2008) 13–23.